The Photocopy Method: Measuring Living Chain Distributions in Radical Polymerization

Erdem Karatekin[1,#], *Ben O'Shaughnessy*[2,*], *Nicholas J. Turro*[1]

[1]Department of Chemistry, Columbia University, New York, NY 10027, USA
[2]Department of Chemical Engineering, Columbia University, New York, NY 10027, USA

[*]To whom correspondence should be addressed (bo8@columbia.edu)
[#]Present address: Institut Curie, Section de Recherche; Laboratoire PCC/UMR 168 11, rue Pierre et Marie Curie; 75231 Paris Cedex 05, France

Summary: We have developed a method to measure living chain molecular weight distributions (MWDs) in free radical polymerization (FRP). By laser photolysis of photoinhibitor molecules included in the polymerizing mixture, the living chains are instantaneously flooded with small molecule radicals carrying fluorescent labels. These radicals react with living chain radical end groups, kinetically freezing growth of living chains and simultaneously end -labelling them: the living chain population has been photocopied. The living MWD is obtained from subsequent analysis by GPC equipped with fluorescence detection. We have measured low conversion thermally initiated PMMA living MWDs. Exponential behaviour is found for large chain length N, in accord with classical Flory-Schultz theory, but at smaller N we establish strong deviations, consistent with the stretched exponential predicted by modern FRP theory incorporating first principles chain length dependencies of termination rate constants. However, this behaviour may derive at least partially from distortions produced by the photocopying technique which can generate power law or logarithmic forms at small N.

I. Introduction: The Importance of the Living MWD

The living chain population is the very heart of linear free radical polymerization [1] (FRP). Living chains are macroradicals, i. e. growing polymer chains with radical end groups at which monomers are added at a certain growth rate v_p (number of monomers added per second; $v_p = k_p\,[mon]$, where k_p is the propagation rate constant and $[mon]$ is the monomer concentration); their growth is the basic polymerization event, as in fig. 1. All other essential properties of FRP such as polymerization rates and molecular weight distributions (MWDs) of the dead chains (the final polymer product; see fig. 2) are determined by the static and kinetic properties of the living chain ensemble.

 CCC 1022-1360/00/$ 17.50+.50/0

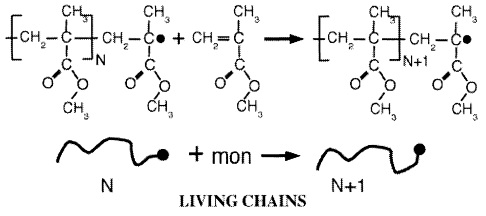

Figure 1: **The polymerization event in a linear FRP is the addition of unsaturated monomer to a living chain, the chain thereby growing from length N to length $N+1$. This continues at rate v_p monomers per second. Poly(methyl methacrylate) (PMMA) is shown as a specific example.**

For this reason, the most basic characteristic of a FRP is the length distribution, or equivalently the MWD, of the living chains: we call this $\psi(N)$, the density of chains having N monomer units. Knowledge of $\psi(N)$ is close to a complete characterization of the living chain engine of FRP. As an experimentalist attempting to unravel the basic mechanisms at play, one would like, more than any other property, to measure this one. Correspondingly, $\psi(N)$ is the natural focus of any fundamental theory of FRP, and it is difficult to verify or refute competing theories without access to this most basic of all properties.

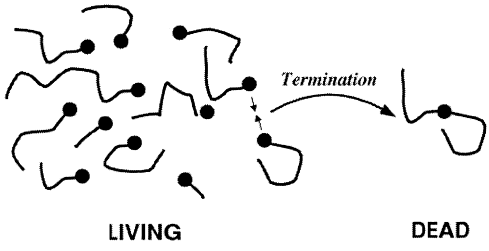

Figure 2: **The family of living chains follows some length distribution $\psi(N)$. Living chains are constantly terminating with one another to produce dead chains, the final product. The form of $\psi(N)$, as well as that of termination rate constants $k(M,N)$, determine the dead MWD. In steady state the total termination rate equals the rate R_i at which new chains are being initiated and $\psi(N)$ settles down to some fixed function.**

Since FRP's invention in the 1930's its great technological significance has inspired a huge research effort and by now measurement of a range of FRP properties has become standard [1–14]. Some of the principal measurements are [1,15,16,13,2]: polymerization rates (using dilatometry, NMR, IR spectroscopy, etc.); dead chain mean length and MWDs (viscometry, gel permeation chromatography–GPC [17]); living chain growth rates v_p (pulsed laser polymerization plus GPC [18–20]); total concentration of living chains (electron paramagnetic resonance [21]; indirectly via v_p and polymerization rates). (One might add to this list living chain lifetimes, τ_{living}, using the "rotating sector method" [1]; this, however, is a model-dependent technique whose measurements are normally interpreted in a Flory-Schulz picture; see below). Conspicuously absent from this list is the living MWD, $\psi(N)$. Whilst the total number of living chains $\psi_{total} \equiv \int_0^\infty dN\, \psi(N)$ is extremely useful, the missing information concerning chain lengths is vital.

Why then has $\psi(N)$ never been measured? Firstly, living chains are highly transient intermediates. With typical values $v_p \approx 10^4$ s^{-1} and mean chain length $\bar{N} \approx 10^3$, their mean lifetime

$$\tau_{living} = \bar{N}/v_p \tag{1}$$

is typically a fraction of a second. This defeats all conventional methods: one simply does not have the time to label and measure the chains in standard ways. A second difficulty is the very tiny concentration of living chains, which are greatly outnumbered by dead chains. Somehow one must distinguish them from their dead chain matrix.

The objective of the work we describe here is the development of a method which can measure $\psi(N)$. We call this the "photocopy method". In the next section we begin by outlining the method.

II. The Photocopy Method

A. The Basic Idea

The essential idea is to instantaneously *freeze* the growth of the living chains kinetically, simultaneously labeling them. Consider a FRP which has reached steady state. Imagine if one could suddenly flood the living chains at some instant with a high concentration of *small* molecule radicals each bearing a fluorescent label. These would react with the radical

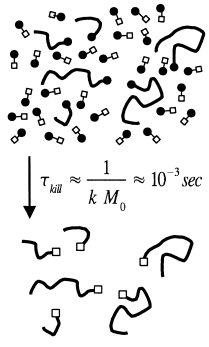

Figure 3: **In the photocopy method the living chains are flooded at some moment with a large excess of small molecule radicals each carrying a fluorescent label (shown square-shaped). These react with the living chain radical ends in a time τ_{kill} which can be made small by choosing high initial concentration of small radicals M_0. Living chain growth is thereby almost instantaneously frozen, and the chains simultaneously labeled: the living MWD has been photocopied.**

end groups of the living chains, freezing chain growth and end-labeling them in the process (see fig. 3). Provided the concentration of small radicals, M, greatly exceeds the total living chain concentration, $P \equiv \psi_{total}$, the small radical kinetics are

$$\frac{dM}{dt} \approx -k_{MM}\,M^2\ , \qquad \frac{M}{M_0} \approx \frac{\tau_{kill}}{t} \quad \text{for} \quad t \gg \tau_{kill} \equiv \frac{1}{k_{MM}M_0} \tag{2}$$

where M_0 is the initial value. Meanwhile we have $dP/dt \approx -k_{MP}MP$ so the long time living chain decay is $P/P_0 \approx (\tau_{kill}/t)^{\lambda}$ where the ratio of rate constants $\lambda \equiv k_{MP}/k_{MM}$ is typically of order unity. Thus, the living chains are killed in a time of order τ_{kill} which, in principle, we can experimentally manipulate to be as short as we like by increasing M_0. If the labeled and frozen living chain population thus created is to be a good representation of the living chain distribution initially present, the kill time must be much less than the intrinsic living chain evolution time scale, τ_{living}:

$$\tau_{kill} \ll \tau_{living} \equiv \frac{1}{k_{PP}P_0} , \qquad \text{or} \qquad M_0 \gg P_0 \qquad \text{(flooding condition.)} \qquad (3)$$

Here the initial concentration of living chains, P_0, is the steady state value and τ_{living} is the intrinsic time for these living chains to decay to zero through self-termination (with rate constant k_{PP}) without external interference. Eq. (3) is the *flooding condition*: we must initially create many more small radicals than the number of macroradicals which are present, in order that during the photocopy window lasting τ_{kill} the living MWD has evolved very little. In practice (see below) we typically achieve $\tau_{kill} \approx 10^{-3}$ s, much less than $\tau_{living} \approx 0.1$ s.

Once this freezing process is complete, we have created a frozen and end-labeled copy of the originally present living MWD: the living chains have been "photocopied". This method copes with (i) the short living chain lifetime problem by virtually instantaneous kinetic freezing of chain growth; (ii) the problem of distinguishing living chains from the dead ones by end-labeling the former which can now be detected selectively from the dead chain background in subsequent analysis by GPC equipped with fluorescence detection as described below, and (iii) the problem of having to measure a very low concentration of living chains by using very sensitive fluorescence detection [22] with highly efficient fluorescent labels. The second and third aspects are as essential as the first.

B. Creating the Small Molecule Radicals: Photoinhibitors

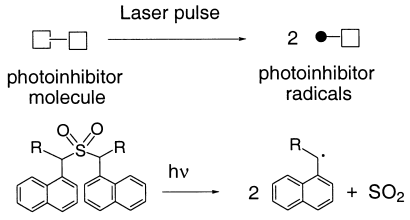

Figure 4:
Top: a photoinhibitor molecule, which does not interfere with the FRP, is photolyzed by a laser pulse to produce "photoinhibitor radicals" which do not attack monomer at substantial rates, are highly reactive toward any radical, and carry a label. Bottom: arylmethyl sulfone compounds, such as DNPMS (R≡-Ph) come close to being ideal photoinhibitors. For discussion of photoinhibitor decomposition products, see refs. 23 and 24.

How can we "instantaneously" generate this flood of small molecule label-bearing radicals? We achieve this with "photoinhibitor" molecules [25,26,23,27,24] which, when laser irradiated at a certain wavelength, photocleave to yield two radicals, each carrying a fluorescent group (see fig. 4). For the idea of photoinhibitors we are greatly indebted to Guillet and co-workers [25,28–30,26,31] who used phototerminating and photoinitiating molecules to control FRPs and end-label polymers.

An *ideal photoinhibitor* has the following properties: (i) It is readily photocleavable to produce radicals; (ii) these radicals are highly reactive towards other radicals and yet (iii) do not react with unpolymerized monomer to initiate new living chains; (iv) the radicals carry a label. Features (ii), (iv) ensure the photoinhibitor radicals readily react with and label the live macroradical ends, while feature (iii) ensures the photocopy is not polluted with extra unwanted labeled living chains generated as in fig. 5.

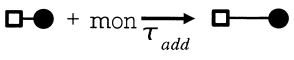

Figure 5: **Non-ideal photoinhibitor radicals attack unpolymerized monomer to initiate new living chains which grow with velocity v_p. Since these carry a fluorescent group (indicated as square-shaped), after termination they contribute to the fluorescence detector signal of the GPC apparatus. For this pollution effect to be small, the mean time to attack a monomer must greatly exceed the living chain lifetime, $\tau_{add} \gg \tau_{living}$ (see text).**

We have searched for a near-ideal photoinhibitor and the best we have found, used in the experiments described below, is di(1-naphthyl, phenyl methyl) sulfone (DNPMS, fig. 4). Upon photolysis using 308 nm laser light, this arylmethyl sulfone compound produces, with good efficiency, two identical radicals with low reactivity toward monomer [23,27,24]. The radicals are derivatives of the naphthylmethyl radical whose reactivity and photophysical characteristics have been studied to some extent [25,28–30,32,33]. Although no data exists in the literature on the rate constants for naphthylmethyl radical addition to alkenes, this is expected to be a "slow" process, since the radical is highly stabilized by the aromatic structure [25,28–30,34,35]. The 1-benzylnaphthyl radicals produced upon photolysis of the photoinhibitor DNPMS, in turn, are expected to be much less reactive than the naphthylmethyl radical, due to their much higher steric constraints and electronic stabilization [34,22]. Generally, τ_{add} depends of course on monomer species and for every new monomer to which one wishes to apply the photocopy method, checks must be made that τ_{add} is sufficiently small. For further detailed discussion on the general issue of photoinhibitor radical addition to alkenes, the reader is referred to ref. 24.

The 1-benzylnaphthyl phototerminator radicals become, upon termination with living chains, excellent fluorescent labels [22,23]. Our GPC fluorescence detector is capable of easily detecting concentrations of the model compound 1-methylnaphthalene as low as 10^{-8} M, at the excitation (300 nm) and emission (350 nm) wavelengths and other typical instrumental settings employed [23,27].

C. The Photocopy Experiment

The overall scheme is shown in fig. 6. The thermally initiated FRP is standard, except for the inclusion of a small concentration of photoinhibitor molecules (DNPMS in the case of the experiments described here). After the FRP reaches steady state a photocopy laser pulse is applied to generate photoinhibitor radicals (M) which kill and label the living chains (P). Note that significant self-recombination of photoinhibitor radicals occurs; our final photocopied MWD must therefore be cut off below a certain molecular weight to avoid counting these spurious species. Note also that homogeneous illumination of the sample volume is not necessary: it is unimportant whether or not the concentration of photoinhibitor radicals, M_0, varies from one position in space to another. All that matters is that the flooding condition is satisfied everywhere. That M_0 varies by a factor of 2 or 3 along the light path is not relevant, provided it is always much greater than the local living chain concentration.

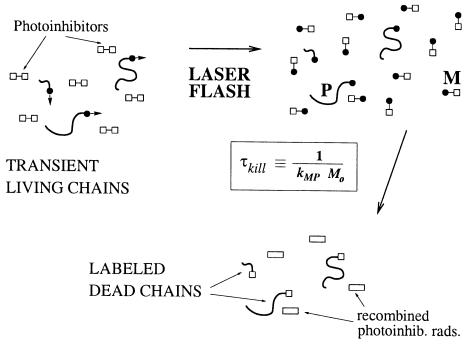

Figure 6: **Scheme of the photocopy method. Included in the FRP are small amounts of photoinhibitor. The system is laser flashed to generate photoinhibitor radicals (M) which label and freeze the growth of the living chains (P) in a time $\tau_{kill} = 1/(k_{MM} M_0) \approx 1/(k_{MP} M_0)$ (recall that $k_{MP} \approx k_{MM}$).**

In fig. 7 the experimental setup is shown. In a typical experiment, 147 mg (9.0×10^{-3} M) of the initiator $2,2'-$azobis(isobutyronitrile) (AIBN) and 20 mg (4.1×10^{-4} M) of the photoinhibitor DNPMS are dissolved in 100 ml neat methyl methacrylate (MMA) monomer. With these concentrations, the absorption of the laser light at 308 nm is negligible for the initiator AIBN and the monomer. 200 μl of the DNPMS/AIBN/MMA mixture is placed in a rectangular clear fused quartz cell with a 0.3 cm pathlength, and argon gas is bubbled through the solution for $\approx$ 5 min to remove oxygen which acts as an inhibitor for FRP. Following degassing, the sealed cell is placed in a thermostat as shown in fig. 7(left) at 60^0C . At this temperature, and at the concentration used, the initiator AIBN decomposes to provide a rate of initiation $R_i \cong 10^{-7}$ M/s. The sample is allowed to polymerize thermally for 2-4 minutes before 5-10 laser shots at 308 nm are applied with a period $t_o \geq 10$ s, much longer than the mean living chain lifetime at steady state, τ_{living}, to build up the labeled living chain concentration. The laser beam is expanded in order to excite the whole sample. Each pulse makes an identical copy, provided the overall conversion ϕ does not change substantially during the pulse sequence. On the other hand the pulses must be separated in time by much more than τ_{living} to allow recovery of the FRP steady state. The FRP is then stopped by taking the polymerization cell off the thermostat. The sample is diluted with solvent before being analyzed using GPC (fig. 7, right) which separates chains according to length N. Our GPC is equipped with a fluorescence (FL) detector which is sensitive *only* to the living chain end labels; in this way the living MWD is measured. Downstream, the analyte then passes through a refractive index (RI) detector which measures all polymers, i. e. essentially measures the dead MWD since dead chains are in enormous excess over the labeled living chains. In this way we are able to measure both the living and dead MWDs simultaneously in a single experiment. Further experimental details are described in refs. 23,27.

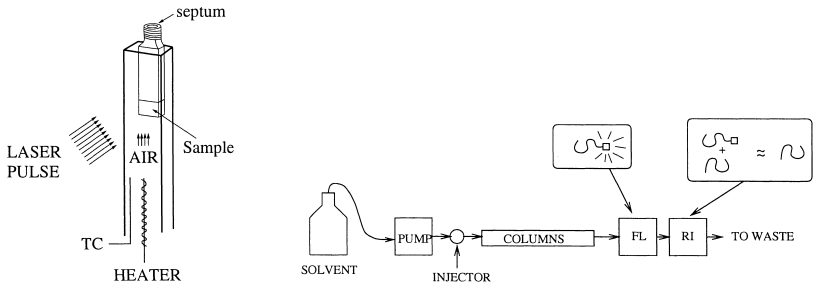

Figure 7: **Photocopy method: experimental setup. Left: A thermally initiated FRP is irradiated with a series of photocopy laser pulses, each (in principle) generating an identical photocopy of the living MWD. Right: The polymerization product is analyzed with GPC apparatus equipped with a fluorescence detector (FL) which measures the fluorescently labeled living chains. This yields the living MWD. A refractive index (RI) detector then measures all chains; since dead chains greatly outnumber the living ones, this yields essentially the dead MWD.**

III. Living MWDs

We have used the photocopy method to measure living MWDs of bulk MMA polymerizations at 60^0C , thermally initiated by AIBN, as described at the end of the previous section. All measurements have been made at *low conversions*, $\phi \lesssim 0.4\%$. A typical raw GPC chromatogram from the FL detector is shown in fig. 8(a). Note the small N (large elution times $\gtrsim$ 24 mins) feature due to recombined photoinhibitor radicals (molecular weight = 435) and intact photoinhibitor (molecular weight = 498) which artifact must ultimately be discarded.

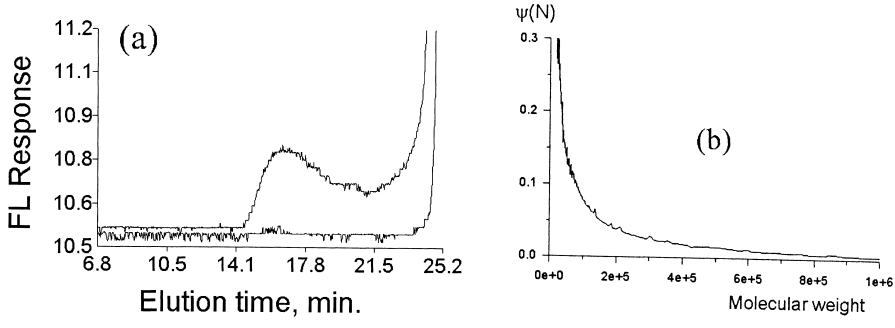

Figure 8: **(a) Typical GPC chromatogram obtained in the photocopy experiment for the DNPMS/AIBN/MMA system using the fluorescence (FL) detector. The chromatogram at the bottom, slightly offset vertically for clarity, is from a DNPMS/AIBN/MMA sample which is subjected only to the thermal FRP part of the experiment (no laser shots). The high amplitude peak starting at about 25 min elution time is due to intact photoinhibitor molecules (molecular weight = 498). (b)** *Number* **molecular weight distribution for the top chromatogram in (a), calculated using molecular weight calibration information [23,27,17].**

With $\bar{N}$ of order 10^3 the loss of, perhaps, $N \lesssim 5$ information is minor; however, it must be subtracted off carefully. After calibration, a typical living MWD is shown in fig. 8(b). To the best of our knowledge, these are the first measured living MWDs in FRP.

The first question one might ask is whether or not our measured MWDs corroborate the classical Flory-Schulz FRP theory [1] dating from the late 1930's. This predicts an exponential form $\psi \sim e^{-N/\bar{N}}$. At a glance, the living MWD of fig. 8(b) appears consistent with this, but for a quantitative assessment we show in fig. 9(a) 11 superposed separately measured living MWDs plotted in log-lin form. For $N \gtrsim 3000$, exponential behavior is indeed rather well obeyed. Clearly, however, there are strong deviations from the classical theory for smaller N. To scrutinize these, in fig. 9(b) we performed a best fit of the small N region with a stretched exponential, $\psi \sim e^{-C(N/\bar{N})^{\beta}}$. Two stretching exponents β were attempted: both $\beta = 0.8$ (with $C = 15$) and $\beta = 0.5$ (with $C = 9$) produce reasonable fits at small N. Meanwhile in fig. 9(c) we attempted a power law fit (data shown in log-log form) to the region $40 \lesssim N \lesssim 2000$, from which we infer a small N behavior $\psi \sim 1/N^{\gamma}$ with $\gamma = 0.88 \pm 0.03$.

In summary: we find exponential behavior $\psi \sim e^{-N/\bar{N}}$ for $N \gtrsim 3000$ with $\bar{N} \approx 3000$. The smaller N data are consistent with: (i) a stretched exponential form $\psi \sim e^{-C(N/\bar{N})^{\beta}}$ (we tried $\beta = 0.8$ and $\beta = 0.5$) and (ii) a power law, $\psi \sim 1/N^{\gamma}$, with $\gamma = 0.88 \pm 0.03$.

We need guidance from theory at this point. What deviations from the classical theory should we expect? To elucidate this, based on a fundamental picture of FRP which incorporates modern advances in polymer physics, we must first think more carefully about the living chain termination processes which govern $\psi(N)$. This is the subject of the following section.

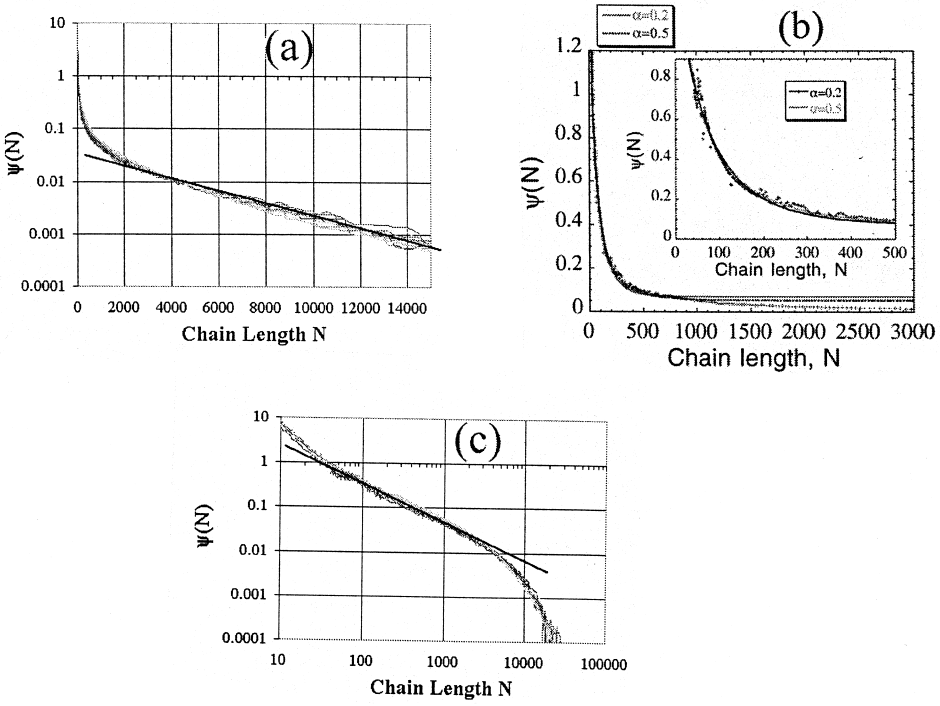

Figure 9: **(a) Living MWD plotted on semi–logarithmic coordinates for the DNPMS/AIBN/MMA system for 11 samples, measured under comparable conditions. The MWDs are vertically shifted to compensate for their different normalizations. The straight line, a linear regression for chain lengths $3,000 < N < 16,000$, has slope $-(2.8 \pm 0.4) \times 10^{-4}$. (b) Short chain part of a representative living MWD measurement (+ signs) for the DNPMS/AIBN/MMA system from (a). Least squares fits of the data for the region $40 < N < 1500$ to a function of the form $c_1 \exp\left(-[N/c_2]^{1-\alpha}\right)$ are also shown, with values of α as indicated ($c_2 \cong 68$ and $c_2 \cong 24$ when $\alpha = 0.2$ and $\alpha = 0.5$ are used, respectively). The inset shows a zoom to smaller scales. (c) Short chain portions of the 11 living MWDs of (a) plotted on double logarithmic coordinates. The straight line, a linear regression for chain lengths $40 < N < 2,000$, has slope -0.884 ± 0.026.**

IV. Dependence of Termination Rate Constants $k(M, N)$ on Chain Lengths

The steady state living MWD $\psi(N)$ results from termination reactions between living chains of all lengths M and N, and so depends strongly on the form of the second order rate constant $k(M, N)$ governing interpolymeric reactions as shown in fig. 10. Here "length" denotes number of monomer units, and each unit is of size a. The classical Flory-Schulz theory [1] approximates k as a constant. However even in dilute solutions (pertinent to

low conversion FRP) there is strong experimental and theoretical evidence for chain-length dependence, albeit a weak one [36–41].

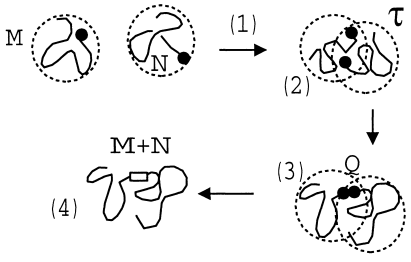

Figure 10: **Polymer-polymer reaction kinetics between chains of lengths N, M bearing reactive end groups. Reaction involves several stages. Center of gravity diffusion must first bring the 2 polymer coils together, process (1). The 2 coils will remain overlapped for a time of order the longest polymer relaxation time τ, stage (2), during which stage small time scale diffusion of the reactive ends may result in repeated reactive group collisions. During each collision, (3), the groups react with probability Q per unit time (for radicals $Q \approx 1/t_a$). If no reaction occurs, the coils separate and must wait for diffusion to collide them with another coil; on the other hand, if one of the collisions results in reaction, the reaction product (4) is generated.**

Thus before attempting to interpret our measured living MWDs, in this section we discuss the form of $k(M, N)$. The discussion is quite general, and has nothing a priori to do with FRP; the reactive end groups, with local reactivity Q (reaction probability per unit time when they are in contact with one another), might be any species (including photoactivated/quencher groups as in phosphorescence quenching studies). Of course our eventual application will be to radicals, where $Q \approx 1/t_a$ is of order the inverse single monomer relaxation time t_a (thus t_a is essentially the time for the reactive end-unit of the chain to diffuse a distance of order its own size a). As a check that this is the right magnitude for Q in the case of radicals, consider the small molecule case ($N = 1$) for which we know $k \approx Qa^3$; then, specializing to radicals, if we set $Q = 1/t_a \approx 10^{10}$ s^{-1} and use $a \approx 3\mathring{A}$ one obtains $k \approx 10^8$ M^{-1} s^{-1}, a typical radical-radical rate constant.

Motivated by our FRP experiments, our interest is the situation where: (i) the reactive chains belong to a very dilute polymer solution, $\phi < \phi^*$, where ϕ is the polymer volume fraction and ϕ^* the overlap threshold [42] at which coils just touch each other; (ii) the solvent is a good swelling one for the chains and (iii) Q is very large, of order $1/t_a$.

We focus on these 3 conditions because: (i) Our FRP measurements are all at low conversion ϕ, and ϕ equals, approximately, the polymer volume fraction in the dead chain solution which is the environment in which living terminations occur; with $\bar{N} \approx 3000$, one has [42] $\phi^* \approx \bar{N}^{-0.8} \approx 0.2\%$. Since our experimental conversions are all $\lesssim 0.4\%$, they fall primarily in the dilute regime, with perhaps a slight extension into semi-dilute conditions.

(ii) MMA is a good solvent for PMMA [43,1,15]. (iii) Radical groups are almost "infinitely" reactive, as discussed above.

Now dilute polymer reaction kinetics in good solvents were studied in refs. 37,38 using first principles renormalization group arguments, and in a much simpler approximate framework in refs. 39,40. But the essential results are very simple to understand, as follows. Consider first a vessel of volume V containing a dilute solution of chains of equal length (i. e. we treat first the case $M = N$) and write $k(N) \equiv k(N, N)$. Now since at any instant the total reaction rate equals Q times the number of chain pairs whose reactive ends are in contact, the number density n of unreacted chains decreases as $-dn/dt = k(N)n^2$ with $k(N) = QVP^{cont}$ where P^{cont} is the probability that any given pair of chains have their reactive ends in contact. In general, due to reactions this is of course *not* equal to the equilibrium contact probability P_{eq}^{cont}. Now for reaction to occur between a given pair, center of gravity diffusion must first bring the polymer coils together (see fig. 10, process (1)). Each such coil-coil collision lasts a total time of order τ (process (2)) where $\tau = t_a(R/a)^3$ is the longest polymer relaxation time and as is well known [42] scales as the coil volume R^3 due to hydrodynamical interactions. Here $R = aN^{0.6}$ is the polymer coil size [42,44] in good solvent. During this collision time τ, small time scale motion of the chain ends must then collide the reactive end groups (process (3)); during each such end-end collision reaction occurs with probability of order Qt_a.

Let us evaluate the total reaction probability during one coil-coil collision lasting τ. Now the fraction of the coil overlap time τ for which the 2 chain end units of size a are in contact can be estimated as the *conditional* equilibrium end-end contact probability, *given* that the 2 coils overlap, namely $P_{eq}^{cont,cond}$. But this is a well known quantity from the theory of self and mutually-avoiding polymers [45–49] and scales as $P_{eq}^{cont,cond} \approx (a/R)^{3+g}$ where $g \approx 0.27$ is des Cloizeaux's "correlation hole" exponent and describes the diminished probability for 2 self and mutually avoiding chains to bring their ends together, relative to the result for ideal coils (for which $g = 0$). Noting each collision lasts t_a, the mean total number of end-end collisions during τ is hence

$$\mathcal{N}_{coll} \approx \frac{\tau}{t_a} P_{eq}^{cont,cond} = \left(\frac{a}{R}\right)^g = \left(\frac{1}{N}\right)^{0.16} \quad . \tag{4}$$

The total reaction probability during one coil-coil encounter, $Qt_a\mathcal{N}_{coll} = Qt_a/N^{0.16}$, is thus very small for large N, *even if* Q *is very large* as for radicals, $Qt_a \approx 1$. Of course, we are interested in very long polymers, $N \gg 1$. Hence coils must undergo many such coil-coil

collisions before reaction occurs; it follows that reactions are a very weak perturbation and, essentially, *equilibrium is unperturbed by the reactions.* Thus the end-end contact probability P^{cont} is essentially the same as its equilibrium value [45–49], $P_{eq}^{cont} = (1/V)(a/R)^g$. Thus $k \approx QVP_{eq}^{cont}$ and for radicals ($Q \approx 1/t_a$) we have

$$k(N) \approx \frac{1}{t_a}\left(\frac{1}{N}\right)^{0.16} \qquad \text{(dilute solution, good solvents.)} \tag{5}$$

The end result is that k scales with N in the same way it would have done for very small Q, i. e. for chemically-controlled reactions[50]. This is very far from a priori obvious, that for large N one should be driven to a "weakly reactive" limit, even when the end groups are themselves virtually infinitely reactive. It necessitates a full treatment of the polymer relaxation kinetics to arrive at this rather counterintuitive conclusion which is true only due to the special circumstances of dilute solution with good solvent. Reactions in concentrated polymer solutions or melts are entirely different: for large Q, reactions are driven for $N \gg 1$ to a *strongly* reacting, diffusion-controlled limit where k has completely different forms to the chemically controlled case. The reader is referred to refs. 37–41,51,52 for detailed systematic calculations.

How does this generalize to $M \neq N$? Similar considerations to those above show that in dilute solutions, good solvent, reactions remain a weak perturbation of equilibrium and $k(M,N) \propto P_{eq}^{cont}$ remains true. But we know that the equilibrium end contact probability between two chains of very different lengths is dominated by the smallest chain [38]. Thus

$$k(M \gg N, N) \equiv k_\infty(N) \sim \left(\frac{1}{N}\right)^{0.16} \quad . \tag{6}$$

What does experiment say? The best to date are probably phosphorescence quenching data [36] which indicate k does decay with a very weak power law. There is also some evidence [53] for small chain domination of k. However, the time scales accessible by these methods are such that it is difficult to probe interpolymeric reactions. Overall, further good experimental measurements of k using novel approaches would be highly desirable, not least for the important application of FRP.

V. Interpreting the Measured Living MWDs

In the previous section we discussed how application of modern polymer physics theories and experiment to reacting polymers has led to the weak scaling forms for $k(M,N)$ shown in eqs. (5) and (6). Returning to FRP, we begin by asking what this implies about steady state living MWDs $\psi(N)$.

A. Modern Theory for $\psi(N)$

In the absence of substantial chain transfer (a good approximation for PMMA [43,1,15]) the time-dependent living MWD $\psi_t(N)$ obeys [54–56]

$$\frac{\partial \psi_t}{\partial t} = -v_p \frac{\partial \psi_t}{\partial N} - H_t(N)\psi_t \ , \qquad H_t(N) \equiv \int_0^\infty dM\, k(M,N)\, \psi_t(M) \tag{7}$$

where the reaction field $H_t(N)$ is the total termination rate for a chain of length N due to all others having any length M. Thus in steady state

$$\psi = \psi_0 \ \exp\left(-\frac{1}{v_p}\int_0^N H(M)\, dM\right) \ . \tag{8}$$

In the Flory-Schulz theory [1] $k(M,N) \to k$ is approximated as constant. Thus $H(N)$ becomes independent of N, and from eq. (8) the living MWD is exponential, $\psi \sim e^{-N/\bar{N}}$. In reality, for low conversion FRP (our case) $k(M,N)$ depends on chain lengths as in eqs. (5) and (6). What then is the form of the reaction field $H(N)$? There are two limits: (1) For large $N \gg \bar{N}$, most M values of importance in the integral defining H are much less than N, so for these $k(M,N) \approx k_\infty(M)$ (see eq. (6)). Thus $H(N) \approx \int_0^\infty dM k_\infty(M)\psi(M)$ is independent of N and ψ is exponential. (2) When N is small, $N \ll \bar{N}$, $k(M,N) \approx k_\infty(N)$ for the relevant M values and we now have $H(N) \approx k_\infty(N) \int_0^\infty dM\, \psi(M) \sim 1/N^{0.16}$. Thus (B,C are constants of order unity)

$$\psi(N) \sim \begin{cases} e^{-B\,(N/\bar{N})^{0.84}} \ , & N \ll \bar{N} \\ \\ e^{-C\,(N/\bar{N})} \ , & N \gg \bar{N} \end{cases} \tag{9}$$

The above result tells us that for large N we expect theoretically to see exponential behavior, as in the Flory-Schulz theory. But for small chain lengths we anticipate strong stretched exponential deviations from the classical theory. Note that this does not in any way indicate that chain length dependence of termination rate constants $k(M,N)$ is stronger at smaller N; N-dependence is true for all lengths (see eqs. (5) and (6)). The large N Flory-Schulz-like behavior results because the termination of a very long chain is dominated by all the much smaller chains with which it can react. The rate constants for these reactions are independent of the length of the long chain. The reader is referred to ref. 57 for further details.

B. Possible Distortions Produced by the Photocopy Method

Before comparing our measured MWDs to theory, we must consider whether or not the photocopy method produces a faithful copy of the actual living MWD. Our aim is to photocopy only the P_0 steady state living chains which were present just before the photocopy laser pulse is applied. There are three potential sources of distortion, each discussed separately below.

(1) Evolution of living chain MWD during the photocopy process. This was already considered in section II. To avoid "blurring" of the actual MWD due to non-instantaneousness of the photocopying process, we saw that the flooding condition, eq. (3), must be satisfied. Our experiments pass this test, since typical values are $M_0 \approx 10^{-6} - 10^{-5}$ M, $P_0 \approx 10^{-8} - 10^{-7}$ M, $\tau_{kill} \lesssim 10^{-3}$ s, $\tau_{living} \approx 0.1$ s.

(2) Initiation of new living chains by non-ideal photoinhibitor radicals. At the instant of the photocopy pulse, the FRP is flooded with photoinhibitor radicals (M) at a concentration perhaps two orders of magnitude greater than that of the living chains initially present, P_0. Hence the number of new "pollutant" living chains (W) initiated by these radicals may be substantial even if the addition time, τ_{add}, is small (fig. 5). Now the total number of pollutants created is $W^{total} = \int_0^\infty dt M(t)/\tau_{add}$, so we can obtain the contribution during the interval $\tau_{kill} < t < \tau_{living}$ by recalling that $M \approx 1/(k_{MM}t)$ during this interval (eq. (2)). Thus

$$\frac{W^{total}}{P_0} \approx \frac{1}{P_0}\int_{\tau_{kill}}^{\tau_{living}} \frac{dt}{\tau_{add}} \frac{1}{k_{MM}t} \approx \frac{\tau_{living}}{\tau_{add}} \ln \frac{\tau_{living}}{\tau_{kill}} \tag{10}$$

after using eq. (3) and the fact that k_{MM} and k_{PP} are of similar order of magnitude. It is simple to show that the contribution from this window in time gives essentially the total

W^{total}. For a good copy, we must have $W^{total} \ll P_0$, i. e. the number of steady state living chains which we aim to photocopy must greatly outnumber the pollutants. Thus we require

$$\tau_{add} \gg \tau_{living} \qquad \text{(good copy.)} \tag{11}$$

This is quite a stringent condition since $\tau_{living} \approx 0.1$ s is rather long. It translates to a second order addition rate constant $k_{add} \lesssim 1\ \mathrm{M}^{-1}\ \mathrm{s}^{-1}$ for a FRP carried out in neat monomer ($[mon] \approx 9$ M), as is the case in our experiments.

In ref. 58 it is shown that these pollutants after termination follow an MWD whose small N behavior is $\psi^{pollutant} \sim 1/N$. This power law will be superposed on the true living MWD, $\psi(N)$. This may conceivably explain the $1/N^{0.88\pm0.03}$ power law fit to our measured living MWDs at small N (fig. 9).

(3) Post-photocopy pulse thermally initiated chains. In reality, directly after a photocopy pulse some new chains will continue to be initiated by the thermal decomposition of the initiator AIBN at rate R_i. A concern is that before the photoinhibitor population (M) has disappeared, sufficient of these post-pulse thermally initiated new living chains ($\mathrm{P}_{thermal}$) will have been created, and then frozen and labeled by M radicals, that they will substantially participate in the final measurements.

Since M is in the great majority, we have $dP^{therm}/dt \approx R_i - k_{MP}MP^{therm}$ whence $P^{therm} = R_i t/(\lambda+1)$ after using the $t > \tau_{kill}$ behavior of $M(t)$ shown in eq. (2). Here $\lambda \equiv k_{MP}/k_{MM}$ is of order unity. Now the rate at which these new thermally initiated chains are capped by M and incorporated into the final photocopy is $k_{MP}MP^{therm} = R_i\lambda(\lambda+1)$. This process continues until $t = \tau_{living}$ by which time $M \approx \lambda P_0$ has dropped to the level of P_0. Thus the total number appearing in the final photocopy is approximately $R_i\tau_{living} \approx P_0$. (The last equality follows because in steady state living chains are produced at rate R_i and last a time τ_{living} before being terminated.) The conclusion is that the number is of the same order as the original number of chains, P_0, which the method sets out to copy. This is a significant source of distortion.

In ref. 58 it is shown that the MWD followed by these thermal pollutants is exponential at large N and diverges weakly at small N, $\psi^{therm} \sim \ln(1/N)$.

VI. Conclusions

We have developed a method to directly measure living MWDs in FRP. For low conversion MMA polymerizations we find an exponential form for the living MWD ψ at large N, but strongly non-exponential behavior at small N. Thus the Flory-Schulz theory, which predicts an exponential form, is not obeyed; this is not surprising given the chain-length dependence of rate constants which are neglected in the classical theory.

The small N behavior is compatible with a stretched exponential, but also with a power law $\psi \sim 1/N^{0.88\pm0.03}$. Since modern theory predicts a stretched exponential, $\psi \sim \exp[-B\,(N/\bar{N})^{0.84}]$, it is tempting to conclude that experiment and theory are in accord. However, the best fits were for stretching exponents somewhat smaller than the theoretical 0.84, and moreover there are possible distortions of the living MWD inherent in the method itself. One potential artifact is due to new living chains initiated by photoinhibitor radicals, which effect we find contributes a $\psi \sim 1/N$ behavior at small N. This is rather close to our best power law fit of $1/N^{0.88\pm0.03}$, so it may be that non-ideality of photoinhibitors underlies the small N measurements. On the other hand, other measurements [23,27,24] suggest this non-ideality is small: we find the total fluorescence intensity (proportional to the total amount of labeled dead chains), as measured in the fluorescence detector of the GPC setup, appears to saturate as photocopy laser flash intensity (proportional to M_o) increases beyond a certain level. If photoinhibitor radical initiation of new chains were important, one would expect the number of labeled dead chains to increase without bound as flash intensity increases and thus creates more M radicals. We cannot entirely exclude, however, that what we measure is actually a very slowly increasing total fluorescence intensity as laser intensity increases; in fact theory predicts a weak logarithmic growth [58].

Another possible cause for the small N form of $\psi(N)$ is post-photocopy pulse thermal initiation of new chains which end up being photocopied along with the steady state living chain MWD of interest. We find this effect pollutes the copy with an amount of chains roughly equal to the number in the MWD of interest, and contributes a weakly divergent $\psi^{therm} \sim \ln(1/N)$ at small N and an exponential at large N. This effect is also therefore a candidate for explaining the data.

A considerable advantage of the method is its ability to measure in a single experiment a large number of distinct FRP properties [27,24] since both living and dead MWDs are

	Photocopy	indep. est.	literature
$\psi(N)$	$\sim \begin{cases} e^{-a_1 (N/\bar{N})^{1-\alpha}} & (N \ll \bar{N}) \\ e^{-a_2 N/\bar{N}} & (N \gg \bar{N}) \end{cases}$ $\alpha \cong 0.2 - 0.5$ * $a_2 = 0.59 \pm 0.04$ $\bar{N} = 2 - 3,000$	-	-
$\overline{N}$	$2,100 \pm 100$	$2{,}800$ [a] $\bar{N}_{dead}/2 \leq \bar{N} \leq \bar{N}_{dead}$	†
ψ_{total} (M)	$2 - 3 \times 10^{-7}$	4×10^{-8} [b]	$\lesssim 10^{-7}$ [c]
v_p (s^{-1})	-	-	6,930 [d]
τ_{living} (s)	0.3 [e]	0.4 [f]	varies
$\overline{N}_{dead}$	$3,300 \pm 200$	$\bar{N} \leq \bar{N}_{dead} \leq 2\bar{N}$	varies
R_p (M/s)	$1 - 2 \times 10^{-3}$ [g]	2.8×10^{-4} [h]	varies
k ($M^{-1}s^{-1}$)	1×10^{7} [i]	6×10^{7} [j]	$10^{6} - 10^{8}$ [k]
f_d	0.43	-	0.46 [k]

Table 1: **Quantities measured in the photocopy experiment (second column, using photoinhibitor DNPMS) and comparison with independent estimates or measurements (third column), or reported values (fourth column), for the FRP of MMA at 60°C initiated with 9×10^{-3} M AIBN ($R_i \cong 10^{-7}$ M/s). $\bar{N}_{dead}$: mean dead chain length; R_p: rate of polymerization; f_d: fraction of living chains terminating via disproportionation.** * Slightly better agreement with larger values of α. $a_1 \approx 15.5$ (9.2) for $\alpha = 0.2$ (0.5). Data for $N \ll \bar{N}$ is also well described by $\psi \sim N^{-\gamma}$, with $\gamma = 0.88 \pm 0.03$. [a] From $\bar{N} = R_p/R_i$, with calculated R_i from known rate of decomposition of AIBN and independently measured R_p. [b] From $\psi_{total} = R_p/v_p$, with R_p from indep. meas., v_p from ref. 20, for pure MMA. [c] Typical values. [d] From ref. 20, for pure MMA. [e] From $\tau_{living} = \bar{N}/v_p$, with $\bar{N}$ from photocopy expt., v_p from ref. 20, for pure MMA. [f] From $\tau_{living} = \bar{N}/v_p$, with $\bar{N}$ from [a], v_p from ref. 20, for pure MMA. [g] From $R_p = v_p \psi_{total}$, with ψ_{total} from the photocopy experiment, v_p from ref. 20, for pure MMA. [h] Measured from slope of ϕ vs polym. time data. ϕ from GPC, RI detection. [i] From $k = 1/(\tau_{living}\psi_{total})$, with τ_{living} and ψ_{total} from photocopy expt. [j] From $k = 1/(\tau_{living}\psi_{total})$, with τ_{living} from [f], ψ_{total} from [b]. [k] Values reported in the Polymer Handbook[43] for FRP of MMA at 60°C . † We are not aware of any previous *direct* measurements of $\bar{N}$.

measured simultaneously (see Table 1). The technique can also probe *non-steady state* properties (see ref. 24); by using photocopy pulses so closely spaced in time that the living MWD has insufficient time to recover to steady state, we are able to track the evolution of the non-steady state MWD from complete annihilation back towards its steady state.

Let us speculate on future applications of the photocopy method and consider how adaptable the technique is. What monomer species are susceptible to our approach? (1) We need monomers which do not absorb significantly at the wavelength used to excite the photoinhibitor (currently 308 nm). (Note that even a small monomer absorption can be a problem since the monomer's concentration greatly exceeds that of photoinhibitor.) We do not view this as a major barrier. For each new monomer species, it may be necessary to tune the excitation wavelength, or in the very worst case to employ a different photoinhibitor. (2) Chain transfer effects. Living chain-monomer transfer is not an issue: this affects the living MWD but does not interfere with its measurement. In fact, in ref. [24] we describe

how non-steady state photocopying experiments in principle allow measurement of chain transfer coefficients by comparing the recovery kinetics of mean chain length (affected by transfer) with total number of living chains (unaffected). On the other hand living chain-photoinhibitor transfer needs to be small and should be checked for each new species by, for example, performing thermal FRPs in the presence and absence of the photoinhibitor molecules (without photolysis) and checking that the dead MWD is unaffected. For MMA we performed this control[23,27,24] and showed this class of chain transfer is unimportant. (3) Photoinhibitor radical disproportionation effects. If "freezing" of living chain growth by photoinhibitor radicals occurs through disproportionation, the living chain though killed is not fluorescently labeled and thus missed from the final living MWD. What matters most here is that disproportionation is not very strongly dominant, since whether a coupling or a disproportionation reaction occurs is (presumably) independent of living chain length to a good approximation (these are highly local effects). This means the same MWD is copied, but with a lower normalization, i. e. the total number of measured living chains is diminished relative to its true value, P_0. Our results for P_0 are close to those independently measured by other methods, suggesting little disproportionation. In summary: this type of disproportionation does not affect the living MWD, though it will diminish the total number of measured living chains.

Finally, the real excitement, both fundamentally and practically speaking, lies at higher conversions. Much of the history of fundamental FRP research has revolved around the issue of entanglements, and we believe the method promises to provide a unique insight into this question by "imaging" the living MWD at high conversions where entanglements must be present. Is this feasible? We see no reason why higher conversions should present insurmountable barriers. Fluorescence conditions may possibly change, but these types of technical issues can in principle be overcome by judicious selection of fluorescence label or conditions for detecting fluorescence. In fact, there are distinct advantages in the much higher living chain concentrations at high conversion, which allow improved separation of the fluorescently labeled living MWD from the dead chain background.

Acknowledgments. This work was supported by the National Science Foundation under grants no. CHE-97-07495, DMR 9816374 and as part of its MRSEC Program under DMR-98-09687. We thank George Lem and Meg Landis for synthesis and characterization of various photoinhibitor molecules and Steffen Jockusch for help with laser equipment. E. K. gratefully acknowledges an Institut Curie post-doctoral fellowship.

References

[1] Flory, P. *Principles of Polymer Chemistry* ; Cornell University Press : Ithaca, New York, 1971.

[2] Moad, G. ; Solomon, D. H. *The Chemistry of Free Radical Polymerization* ; Elsevier Science : Tarrytown, New York, 1995.

[3] Rempp, P. ; Merrill, E. *Polymer Synthesis* ; Huethig & Wepf : New York, 1986.

[4] Bamford, C. H. ; Barb, W. G. ; Jenkins, A. D. ; Onyon, P. F. *The Kinetics of Vinyl Polymerization by radical Mechanisms* ; Butterworths : London, 1958.

[5] Benson, S. W. ; North, A. M. *J. Am. Chem. Soc* **1962**, *84*, 935–940.

[6] Ito, K. *J. Polym. Sci.: Polym. Chem. Ed.* **1974**, *12*, 1991–2004.

[7] Mahabadi, H.-K. *Macromolecules* **1985**, *18*, 1319–1324.

[8] Mahabadi, H.-K. *Macromolecules* **1991**, *24*, 606–609.

[9] Cardenas, J. ; O'Driscoll, K. F. *J. Polym. Sci., Polym. Chem. Ed.* **1976**, *14*, 883–897.

[10] Tulig, T. J. ; Tirrell, M. *Macromolecules* **1981**, *14*, 1501–1511.

[11] Tulig, T. J. ; Tirrell, M. *Macromolecules* **1982**, *15*, 459–463.

[12] Russell, G. T. ; Napper, D. H. ; Gilbert, G. *Macromolecules* **1988**, *21*, 2133–2140.

[13] Bamford, C. H. in *Encyclopaedia of Polymer Science and Engineering Vol. 13* chapter 'Radical Polymerization' edited by Marks, H. F. ; Bikales, N. M. ; Overberger, C. G. ; Menges, G. ; Kraschwitz, J. I. (John Wiley & Sons New York 1985).

[14] Morawetz, H. *Polymers, the Origins and Growth of a Science* ; John Wiley & Son : New York, 1985.

[15] Odian, G. *Principles of Polymerization* ; John Wiley and Sons : New York, 1981.

[16] Rabek, J. F. *Experimental Methods in Polymer Chemistry: Physical Principles and Applications* ; John Wiley & Sons : New York, 1980.

[17] Yau, W. W. ; Kirkland, J. J. ; Bly, D. D. *Modern Size–Exclusion Liquid Chromatography: Practice of Gel Permeation and Gel Filtration Chromatography* ; Wiley : New York, 1970.

[18] Buback, M. ; ; Gilbert, R. G. ; Hutchinson, R. A. ; Klumperman, B. ; Kuchta, F.-D. ; Manders, B. ; O'Driscoll, K. F. ; Russell, G. T. ; Schweer, J. *Macromol. Chem. Phys.* **1995**, *196*, 3267–3280.

[19] Olaj, O. F. ; Bitai, I. ; Hinkelmann, F. *Makromol. Chem.* **1987**, *188*, 1689–1702.

[20] Hutchinson, R. A. ; Aronson, M. T. ; Richards, J. R. *Macromolecules* **1993**, *26*, 6410–6415.

[21] Kamachi, M. *Adv. Polym. Sci.* **1987**, *82*, 207–275.

[22] Turro, N. J. *Modern Molecular Photochemistry* ; University Science Books : Mill Valley, California, 1991.

[23] Karatekin, E. *Dynamics of Free Radical Polymerization.* PhD thesis Columbia University New York, NY 1999.

[24] Karatekin, E. ; Landis, M. ; Lem, G. ; O'Shaughnessy, B. ; Turro, N. J. *Macromolecules* **2001**, *34*, 8202–8215.

[25] Holdcroft, S. ; Yuen, K. H. ; Guillet, J. E. *J. Polym. Sci.: Part A: Polym. Chem.* **1990**, *28*, 1495–1505.

[26] Tang, B.-Z. ; Holdcroft, S. ; Guillet, J. E. *Macromolecules* **1994**, *27*, 5487–5490.

[27] Karatekin, E. ; Landis, M. ; Lem, G. ; O'Shaughnessy, B. ; Turro, N. J. *Macromolecules* **2001**, *34*, 8187–8201.

[28] Holdcroft, S. ; Guillet, J. E. *J. Polym. Sci.: Part A: Polym. Chem.* **1991**, *29*, 729–737.

[29] Holdcroft, S. ; Tang, B.-Z. ; Guillet, J. E. *J. Chem. Soc.,Chem. Commun.* **1991**, pages 280–282.

[30] Holdcroft, S. ; Guillet, J. E. *Macromolecules* **1991**, *24*, 1210–1212.

[31] Modi, P. J. ; Guillet, J. E. *J. Photochem. Photobiol. A: Chem.* **1994**, *84*, 213–220.

[32] Johnston, L. J. ; Scaiano, J. C. *J. Am. Chem. Soc.* **1985**, *107*, 6368–6372.

[33] Horspool, W. ; Armesto, D. *Organic Photochemistry: A Comprehensive Treatment* ; Ellis Horwood PTR Prentice Hall : New York, 1992.

[34] Fischer, H. in *Factors Controlling the Addition of Carbon Centered Radicals to Alkenes and Alkynes* pages 63–78 edited by Minisci, F. (Kluwer Dordrecht 1997) Vol. 27 of *NATO ASI Series. Partnership sub-series 3, High technology.*

[35] Modi, P. J. ; Guillet, J. E. ; Scaiano, J. C. ; Wintgens, V. *J. Photochem. Photobiol. A: Chem.* **1994**, *81*, 87–91.

[36] Mita, I. ; Horie, K. *J. Macromol. Sci., Rev. Macromol. Chem. Phys.* **1987**, *C27(1)*, 91–169.

[37] Friedman, B. ; O'Shaughnessy, B. *Europhys. Lett.* **1993**, *23*, 667–672.

[38] Friedman, B. ; O'Shaughnessy, B. *Macromolecules* **1993**, *26*, 5726–5739.

[39] O'Shaughnessy, B. *Phys. Rev. Lett.* **1993**, *71*, 3331–3334.

[40] O'Shaughnessy, B. *Macromolecules* **1994**, *27*, 3875–3884.

[41] Friedman, B. ; O'Shaughnessy, B. *Int. J. Mod. Phys. B* **1994**, *8*, 2555–2591.

[42] de Gennes, P. G. *Scaling Concepts in Polymer Physics* ; Cornell Univ. Press : Ithaca, New York, 1985.

[43] Brandrup, J. ; Immergut, E. H. ; Grulke, E. A. ; Abe, A. ; Bloch, D. R. *Polymer Handbook*, 4th ed., ; Wiley : New York, 1999.

[44] Doi, M. ; Edwards, S. F. *The Theory of Polymer Dynamics* ; Clarendon Press : Oxford, 1986.

[45] des Cloizeaux, J. *Phys. Rev. A* **1974**, *10*, 1665.

[46] des Cloizeaux, J. *J. Phys. (Paris)* **1980**, *41*, 223.

[47] Witten, T. A. ; Prentis, J. J. *J. Chem. Phys.* **1982**, *77*, 4247.

[48] Lapp, A. ; Mottin, M. ; Strazielle, C. ; Broseta, D. ; Leibler, L. *J. Phys. II (Paris)* **1992**, *2*, 1247.

[49] Kruger, B. ; Schafer, L. ; Baumgartner, A. *J. Phys. (Paris)* **1989**, *50*, 3191.

[50] Khokhlov, A. R. *Makromol. Chem., Rapid Commun.* **1981**, *2*, 633.

[51] M.Doi *Chem. Phys.* **1975**, *11*, 107–113, 115–121.

[52] de Gennes, P. G. *J. Chem. Phys.* **1982**, *76*, 3316–3321, 3322–3326.

[53] Wisnudel, M. D. ; Torkelson, J. M. *J. Polym. Sci., Polym. Phys. Ed.* **1996**, *34*, 2999.

[54] O'Shaughnessy, B. ; Yu, J. *Macromolecules* **1994**, *27*, 5067–5078.

[55] O'Shaughnessy, B. ; Yu, J. *Macromolecules* **1994**, *27*, 5079–5085.

[56] O'Shaughnessy, B. ; Yu, J. *Phys. Rev. Lett.* **1994**, *73*, 1723–1726.

[57] B. O'Shaughnessy, preprint.

[58] Karatekin, E. ; O'Shaughnessy, B. ; Turro, N. J. **2000**, *"Theory of Photocopying Living Chain Distributions"*, preprint.